International Journal of Thermophysics, Vol. 21, No. 5, 2000

Apparatus for Measuring Vapor-Liquid Equilibria and Phase Densities of Complex Aqueous Solutions

L. A. Watts[1, 2] and B. Louie[1]

Received March 3, 2000

A new apparatus has been designed and constructed to measure the vapor-liquid equilibria and phase densities of corrosive, complex aqueous solutions containing organic solvents and salts. The apparatus is designed for isothermal operation from ambient temperatures to 400 K. Phase equilibrium measurements at higher temperatures may be achieved without density measurements. This paper presents a detailed description and performance testing of the apparatus. Measurements of the vapor pressures and saturated liquid densities of ethanol and the vapor pressure of an ethanol-water mixture ($x_{ethanol} = 0.6743$ mole fraction) from 308 to 385 K at pressures to 15 MPa are used as performance tests.

KEY WORDS: azeotrope; corrosive; density; ethanol; mixture; salts; vapor-liquid equilibria; VLE; vapor pressure.

1. INTRODUCTION

The measurement and prediction of the properties of complex aqueous solutions containing organic solvents and salts are needed to provide data for the design of separation processes. Distillation is a commercially successful process for separating binary systems having different boiling points. However, for systems of components having close boiling points, azeotropes, or other aqueous-electrolyte systems which are difficult to separate, binary distillation often cannot produce a high-purity product stream. In these cases, an additive can act as a separating agent. This approach is known as extractive or azeotropic distillation. For instance, adding phenol to the distillation of toluene-methylcyclohexane enables the extraction of

[1] Physical and Chemical Properties Division, National Institute of Standards and Technology, 325 Broadway, Boulder, Colorado 80305, U.S.A.

[2] To whom correspondence should be addressed.

0195-928X/00/0900-1139$18.00/0

toluene from the binary mixture and results in a high-purity product of methylcyclohexane. The addition of salt to an aqueous-organic azeotrope can be used to facilitate separation of the water and the organic component. The salt can decrease the solubility of the organic in the aqueous solution and increase its vapor pressure over the solution. The boiling point is shifted, making separation by distillation possible.

Aqueous waste solutions containing organic solvents and salts present difficult environmental treatment and characterization problems. Traditionally, the models available for systems like these have been limited to liquid-phase chemistry, ignoring the coexisting equilibrium vapor present. The lack of comprehensive and accurate predictive models for the properties of mixed aqueous wastes represents a severe deficiency in the fundamental knowledge necessary to enable remediation efforts. Phase equilibrium measurements are essential for the development of accurate models for not only the liquid- and vapor-phase composition, but also the phase densities.

This paper describes a new corrosion-resistant experimental apparatus that provides accurate measurements of the phase compositions, densities, and pressures of aqueous organic-salt or mixed-solvent electrolyte solutions over a wide range of temperatures, pressures, and compositions.

2. EXPERIMENTAL APPARATUS

The new vapor-liquid equilibrium (VLE) apparatus consists of an equilibrium cell, vapor and liquid densimeters, pumps for recirculation, pressure and temperature transducers, and a gas chromatograph (GC) sampling system. A diagram of the apparatus is shown in Fig. 1. The furnace contains the vapor pump, the GC sampling valve, and an aluminum block housing the equilibrium cell and the densimeters. These are illustrated in the lower half of Fig. 1. The liquid pump, pressure transducers, and sample reservoir are located on the furnace lid (upper part of Fig. 1), along with the valves and tubing for the GC and for vacuum and liquid recirculation. These components are linked to the rest of the apparatus inside the furnace through an insulated piping feedthrough.

The central piece of the equipment is a thick-walled pressure vessel used as the equilibrium chamber. The 300 ml cell, 0.16 m OD $\times$ 0.25 m long, is made of Hastelloy C-276[3] to withstand potentially corrosive conditions. The cell is rated to 70 MPa and 700 K. The equilibrium cell is connected to the rest of the system with 1.5 mm (ID) tubing of the same alloy

[3] Brand names and commercial sources of material and instruments when noted, are given for scientific completeness. Such information does not constitute a recommendation by the National Institute of Standards and Technology nor does it suggest that those products or instruments are the best for the described application.

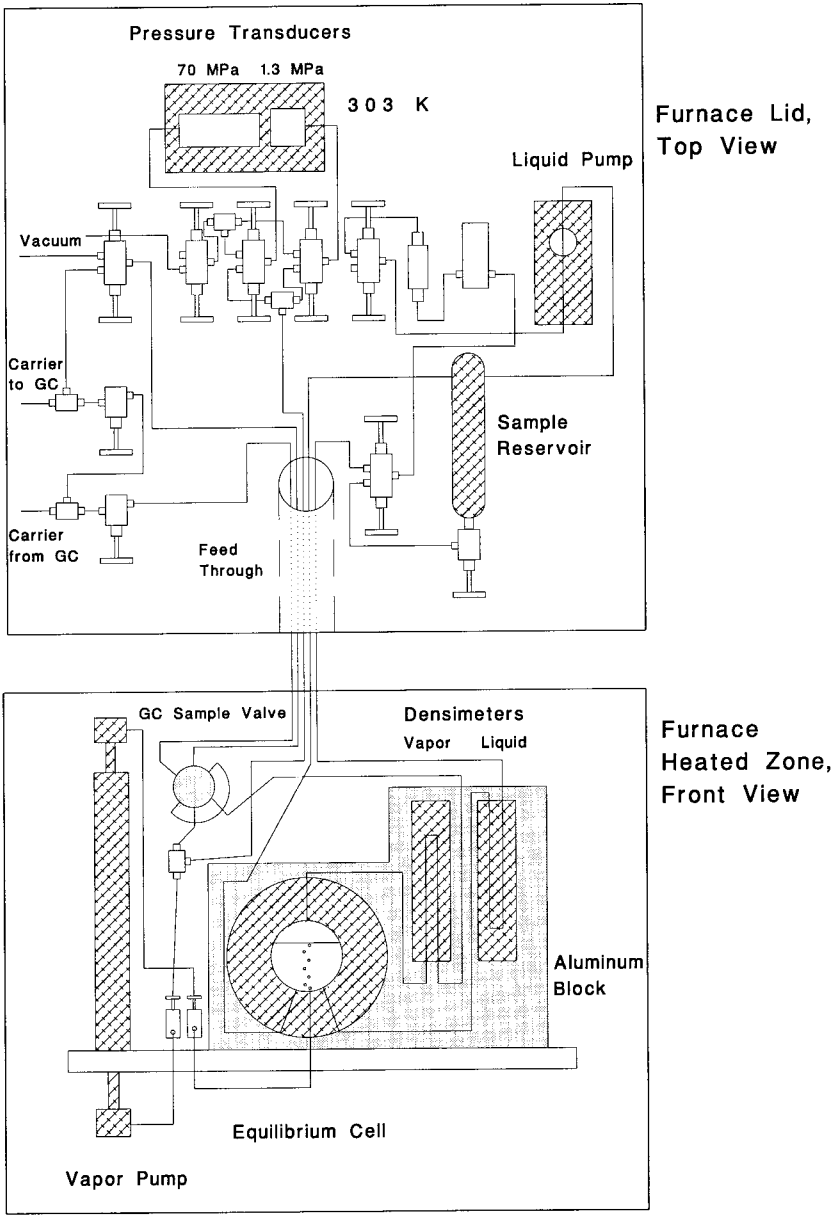

Fig. 1. Schematic of the vapor-liquid equilibrium apparatus for complex aqueous solutions.

as the pressure vessel. The cylindrical cell is placed horizontally in the apparatus. In this position, ports on the top and bottom of the chamber enable removal of small volumes of vapor and liquid for sampling and re-circulation to the cell. One end of the cell has a bolted closure with a sapphire viewing port, which is sealed by a spring-loaded, polymer filled PTFE gasket. This sapphire window enables a visual determination of an adequate volume of fluid within the cell and confirmation of specific operating procedures such as fluid recirculation. The window is replaced with a disk of the same alloy as that of the main cell when a system corrosive to sapphire is under study.

Vapor and liquid densities are measured with commercially available, vibrating tube densimeters. The vapor densimeter's operating range is from 0 to 20 MPa (0 to 3000 psi) at temperatures up to 400 K. The liquid densimeter's operating range is from 0 to 70 MPa (0 to 10000 psi) at temperatures up to 425 K. The manufacturer states that the overall uncertainty of a density measurement is $\pm 0.5\ \mathrm{kg \cdot m^{-3}}$. An aluminum block surrounds the equilibrium cell and densimeters to minimize thermal gradients between these components.

The apparatus is suspended in a high-temperature, forced-air convection furnace. The furnace temperature is controlled with a proportional-integral-derivative (PID) controller that uses a 100 Ω platinum resistance thermometer (PRT) as input. This PRT is located in the airspace in front of the apparatus. The temperature is measured at various locations on the apparatus by a 25 Ω standard PRT, two 100 Ω PRTs, and a 500 Ω PRT. These measurements allow careful monitoring of the temperature during heating and cooling, and of the temperature gradients in the apparatus. The air temperature in the furnace is measured using the 500 Ω PRT located above the apparatus, and, at equilibrium, it varies by less than ± 0.1 K from the set temperature. The cell temperature is measured with a 25 Ω ITS-90-calibrated standard PRT inserted into a thermal well that runs half the length of the outer wall of the cell. This standard PRT has a typical stability of 0.001 K per year for these operating conditions. The equilibrium cell temperature varies by less than ± 0.005 K over the course of data collection (typically 20 minutes). Two calibrated PRT sensors with a resolution of ± 0.001 K and in good thermal contact with the densimeters measure the temperatures of each unit. These PRTs are calibrated independently at NIST against the 25 Ω ITS-90 standard PRT. Type E differential thermocouples showed that the temperature gradients across the aluminum block are less than 0.002 K at equilibrium.

Vapor and liquid recirculation is performed to mix the cell contents, fill the densimeters with the equilibrated phases, and to supply fresh vapor for sampling. Vapor recirculation is accomplished with a magnetically-driven

piston pump located in the furnace. The liquid recirculation pump, located on the furnace lid, is a piston-type metering pump. A six-port GC sample valve located in the furnace is used for sampling of the vapor phase. The molar composition has an overall uncertainty of 0.005 mole fraction as determined by repeated measurements of gravimetrically prepared binary standard mixtures. Condensation in the vapor lines in the furnace outside the aluminum block is prevented by the wrapping of the lines with heating tape to maintain a 2 K differential temperature above the furnace temperature. Heating of the lines outside the furnace provides preheating to the GC column. These lines are well insulated to minimize the temperature gradients in the oven.

Cell pressures are determined using two quartz pressure transducers, each having an uncertainty, as stated by the manufacturer, of $\pm 0.01\%$ over their range. These transducers are located on the furnace lid (upper part of Fig. 1) in a temperature-controlled enclosure maintained at 303 K. Vertical portions of the line to the pressure transducers are heat-traced to avoid the formation of liquid in the lines. The horizontal portions of the lines near the transducers are allowed to remain at room temperature as liquid in this portion of the line will not effect the pressure reading. The low-pressure transducer has a range between 0 and 1.4 MPa, and the high pressure transducer has a range between 0 and 70 MPa. The pressure transducers are calibrated against NIST-traceable dead-weight pressure balances, and the vacuum reading is checked before each sample is run.

3. DENSIMETER CALIBRATION

The liquid and vapor vibrating-tube densimeters were calibrated using an empirical equation that relates the measured vibrational period, temperature, and pressure to the density. The general calibration equation for density (ρ) as a function of temperature (T; K), pressure (P; MPa) and vibrational period (τ) is [1, 2]:

$$\rho(T, P) = \beta_1 + \beta_2 T + \beta_3 P + (\beta_4 + \beta_5 T + \beta_6 T^2) \left(\frac{\tau(T, P)}{\tau(T_0, 0)} \right)^2 \tag{1}$$

where β_i are the calibration constants unique for each densimeter, $\tau(T, P)$ is the measured vibrational period, and $\tau(T_0, 0)$ is the vibrational period at the selected reference temperature (T_0) in vacuum. The densimeters were calibrated over the operating range of temperatures and pressures with vacuum, nitrogen, and water as reference systems. Ultra-high-purity nitrogen (99.9995%) and distilled, deionized and degassed water with a resistance of greater than 18 MΩ/cm were used for calibration fluids.

Nitrogen was used for the low-density range, up to 160 $kg \cdot m^{-3}$ at 15 MPa. The equation of state from Younglove [3] was used to obtain the nitrogen density at the measured temperature and pressure. Liquid water was used to extend the calibration to high density (1000 $kg \cdot m^{-3}$). The equation of state of Hill [4] was used to determine the density of water for the measurement conditions. The measurements were performed over the range of temperatures from 308 to 385 K and at pressures from 0 to 17 MPa. The deviations of the measured data and calculated densities from Eq. (1) are given as a function of temperature for the liquid densimeter in Fig. 2, and the same deviations are plotted as a function of pressure in Fig. 3. Very similar results were obtained for the vapor densimeter.

The density calculated from the measured period, temperature, and pressure can have two sources of error. The first is from the equation itself, which is an approximation of the effects of pressure and temperature on a vibrating tube [2]. The second is from the measurement errors of the temperature, pressure, and period. An analysis of the propagation of uncertainty in the temperature, pressure, and period reading on the density value found that the density may vary by 0.06 $kg \cdot m^{-3}$ through these combined uncertainties. The standard deviation of the density is 0.17 $kg \cdot m^{-3}$, and

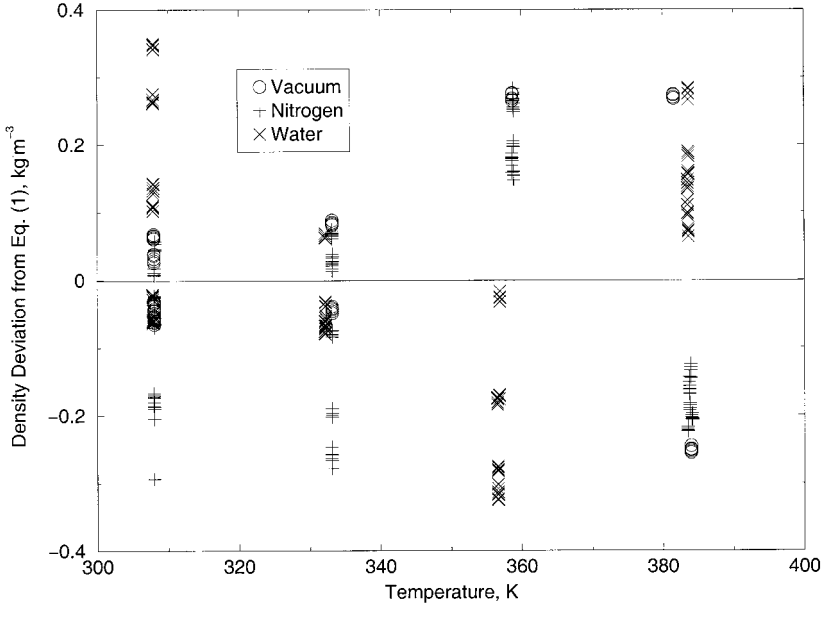

Fig. 2. Density deviation ($\rho_{measured} - \rho_{calculated}$) as a function of temperature for the liquid densimeter calibration using Eq. (1) with vacuum, nitrogen, and water.

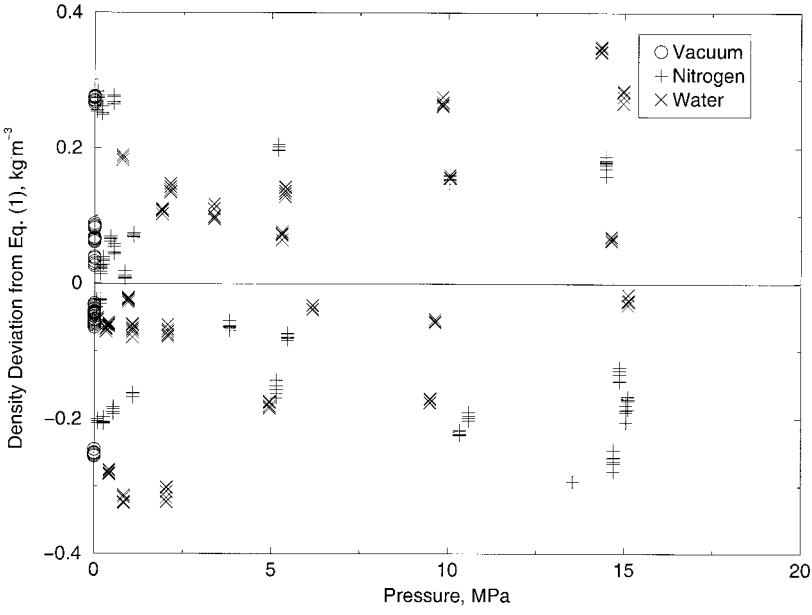

Fig. 3. Density deviation ($\rho_{\text{measured}} - \rho_{\text{calculated}}$) as a function of pressure for the liquid densimeter calibration using Eq. (1) with vacuum, nitrogen, and water.

the maximum deviation is $\pm 0.35\ \text{kg} \cdot \text{m}^{-3}$. Moreover, within each data set the values are reproducible to within $0.05\ \text{kg} \cdot \text{m}^{-3}$, in agreement with the propagation of uncertainty analysis. The trend of the data in each figure demonstrates an absence of bias with respect to temperature or pressure.

4. EXPERIMENTAL

Vacuum readings for the pressure transducers are recorded for each isotherm. For VLE measurements, the system is filled approximately three-quarters full with a pure liquid or a gravimetrically prepared mixture. The liquid and vapor recirculation pumps are started in order to ensure thorough mixing and filling of the densimeters. Once thermal equilibrium is achieved, the recirculation is stopped, the pressure and temperature are recorded, and the composition of the vapor phase is measured. A sample for measurement is obtained with a six-port GC valve located in the furnace. The vapor sample is pulled into the sample loop using the vapor pump, then injected into the GC by manually switching in the carrier gas stream. The temperature is increased to the next point of interest, and the system again is allowed to attain equilibrium. The system may also be used

Table I. Vapor Pressure for Ethanol: T, Temperature (ITS-90); P, Measured Vapor Pressure; $P_{\text{calculated}}$, Calculated Vapor Pressure from Ambrose and Sprake [6] Refit to ITS-90 Temperatures; Deviation $= P - P_{\text{calculated}}$

T (K)	P (MPa)	$P_{\text{calculated}}$ (MPa)	Deviation (MPa)
308.171	0.013835	0.013778	0.000057
308.171	0.013831	0.013778	0.000053
308.169	0.013829	0.013776	0.000053
308.171	0.013828	0.013778	0.000050
308.169	0.013823	0.013776	0.000047
367.991	0.188210	0.188370	−0.000159
383.741	0.319874	0.320011	−0.000137
373.011	0.223558	0.224351	−0.000793
352.092	0.104010	0.104062	−0.000052
341.996	0.068862	0.068982	0.000120
331.651	0.043915	0.043894	0.000021
362.347	0.153847	0.153681	0.000166

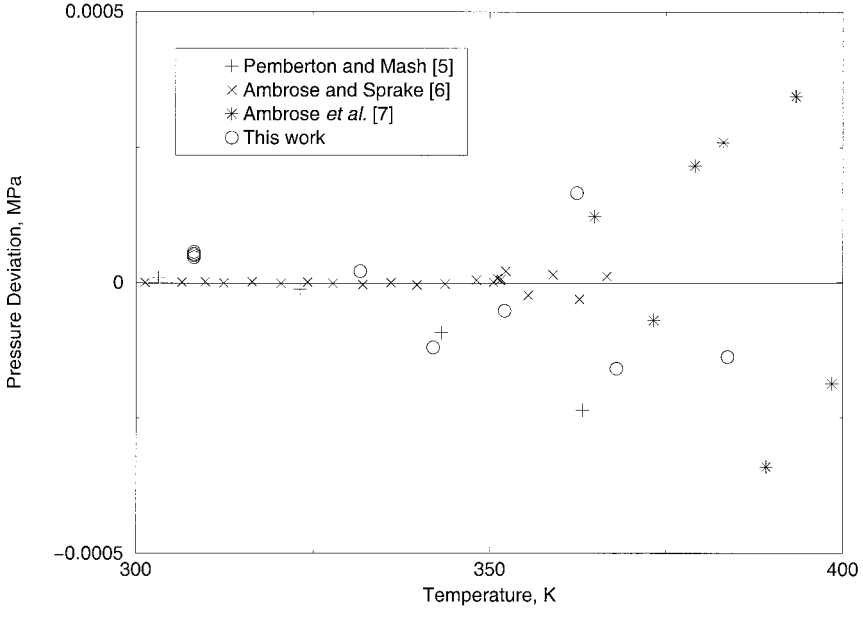

Fig. 4. Deviation of the ethanol saturation pressure ($P_{\text{measured}} - P_{\text{calculated}}$) from the equation of Ambrose and Sprake [6], refitted to converted ITS-90 temperatures.

Table II. Liquid Densities of Ethanol: T, Temperature (ITS-90); P, Pressure; ρ, Measured Liquid Density; $\rho_{\text{calculated}}$, Liquid Density Calculated using Cibulka [8] and Cibulka and Zikova [9]; Deviation $= \rho - \rho_{\text{calculated}}$

T (K)	P (MPa)	ρ ($kg \cdot m^{-3}$)	$\rho_{\text{calculated}}$ ($kg \cdot m^{-3}$)	Deviation ($kg \cdot m^{-3}$)
308.169	0.01381	776.10	776.33	−0.23
318.256	0.02436	767.12	767.43	−0.31
333.313	0.05021	753.37	753.74	−0.37
358.702	0.13971	728.97	729.10	−0.11
358.726	0.14394	728.75	729.07	−0.32
368.019	0.19047	719.14	719.35	−0.21
383.786	0.31972	701.63	701.77	−0.14
372.953	0.22292	713.66	714.01	−0.35
308.116	0.19181	776.10	776.53	−0.44
308.134	0.52465	776.40	776.83	−0.43
308.159	0.74217	776.62	777.01	−0.39
308.122	0.89966	776.80	777.19	−0.39
308.084	1.96888	777.83	778.21	−0.38
308.106	5.09576	780.67	781.01	−0.35
308.174	9.88582	784.87	785.13	−0.26
308.165	14.88606	789.06	789.29	−0.23
318.271	0.11844	767.15	767.50	−0.35
318.241	0.84364	767.91	768.25	−0.35
318.288	1.06122	768.09	768.43	−0.33
318.291	1.84871	768.89	769.20	−0.31
318.274	4.84402	771.86	772.11	−0.25
318.238	9.3544	776.12	776.32	−0.20
318.234	11.86553	778.38	778.57	−0.19
333.277	0.27975	753.62	754.03	−0.41
333.284	0.56112	753.94	754.34	−0.40
333.268	0.98874	754.44	754.82	−0.38
333.259	1.92305	755.48	755.85	−0.37
333.248	4.85905	758.68	758.99	−0.31
333.304	9.11501	762.93	763.27	−0.34
333.323	13.8923	767.59	767.89	−0.30
358.71	0.38145	729.09	729.41	−0.32
358.713	0.76594	729.60	729.92	−0.32
358.703	1.13548	730.08	730.42	−0.34
358.675	2.43728	731.95	732.16	−0.21
358.58	4.69598	734.84	735.14	−0.30
358.806	9.52066	740.42	740.78	−0.36
358.784	14.76053	746.38	746.73	−0.35

for single-phase density and PVT measurements by filling completely with the fluid of interest to the desired pressure.

5. PERFORMANCE TESTS

The performance of the apparatus was verified with measurements on pure ethanol and an ethanol-water mixture. The ethanol used for the measurements had a stated purity of 99.5% or greater. This purity was confirmed with GC-mass spectrometry analysis. Less than 0.5% water was detected, and the ethanol was used without further purification. The vapor pressures were measured over the range of temperatures from 308 to 385 K. Table I presents measurements of the vapor pressure of ethanol for this study, and these data are compared with other results in Fig. 4. These measurements are compared to those of Pemberton and Mash [5], Ambrose and Sprake [6], and Ambrose et al. [7] using the vapor pressure equation of Ambrose and Sprake [6]. The data of the other studies were first converted to the ITS-90 temperature scale, and the Ambrose and Sprake [6] equation was re-fit to the original data. The vapor pressures

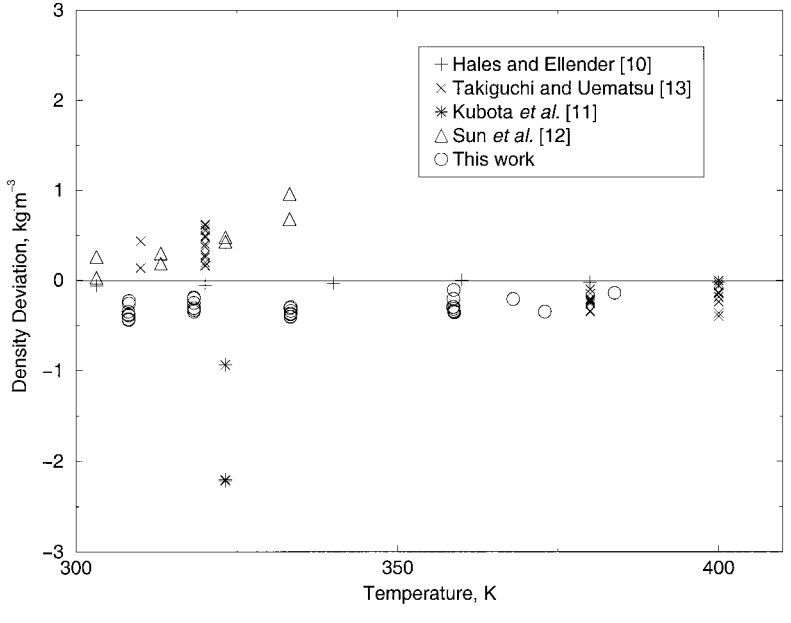

Fig. 5. Ethanol liquid density deviation ($\rho_{\text{measured}} - \rho_{\text{calculated}}$) as a function of temperature for measured values compared to the equations of Cibulka [8] and Cibulka and Zikova [9].

were measured with the low-range pressure transducer, which has an uncertainty of 0.01% or ± 0.00014 MPa. The calculated deviations from this work are comparable to those of other studies, and lie within the uncertainty of the pressure measurements.

Table II presents the liquid density measurements over the range of pressures from saturation to 15 MPa at temperatures from 308 to 385 K. The liquid density deviation values as a function of temperature and pressure are presented in Figs. 5 and 6, respectively. The current data are compared to those of other studies by using deviations from the calculated values of the saturated-liquid density of Cibulka [8], and the liquid densities at elevated pressures of Cibulka and Zikova [9]. These measured liquid density deviations from this work, shown in Figs. 5 and 6, appear systematically lower than those of other studies [10–13]. However, the values are all within the uncertainty of the density measurements. Furthermore, these small deviations do not exhibit either a temperature or pressure bias over the respective range of values.

The vapor pressure and vapor composition were measured for a liquid mixture of ethanol-water with a composition of 0.6743 mole fraction

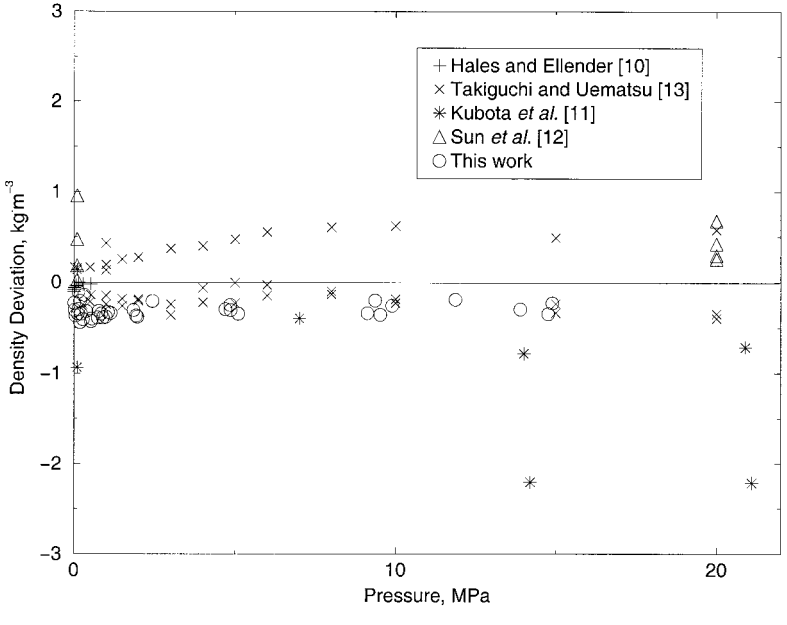

Fig. 6. Ethanol liquid density deviation ($\rho_{\text{measured}} - \rho_{\text{calculated}}$) as a function of pressure for measured values compared to the equation of Cibulka [8] and Cibulka and Zikova [9].

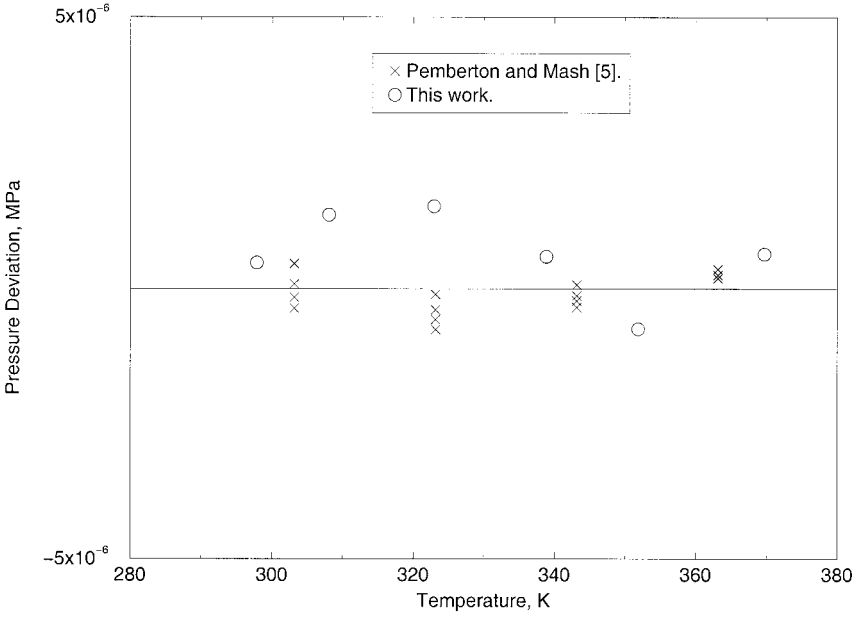

Fig. 7. Pressure deviation ($P_{\text{measured}} - P_{\text{calculated}}$) as a function of temperature for ethanol water mixtures compared to the Peng–Robinson–Stryjek–Vera [14] equation of state with Wong–Sandler [15] mixing rules.

ethanol. The measured vapor pressures are compared to similar compositions (0.50 to 0.72 liquid mole fraction ethanol) measured by Pemberton and Mash [5] in Fig. 7. The deviation values are obtained by comparing the measured results to predicted values using the Peng–Robinson–Stryjek–Vera [14] equation of state with the Wong–Sandler [15] mixing rules. The pressure deviations are even less than those for pure ethanol, and agree well with published data. The vapor composition measurements were within ± 0.01 mole fraction of the predicted values for this work and ± 0.03 mole fraction for Pemberton and Mash [5].

6. CONCLUSION

An apparatus has been developed for measuring the vapor-liquid equilibria of mixtures containing water, miscible organic solvents, and salts. Systems may be measured from ambient temperatures to 400 K, and to 700 K without density measurement. The overall uncertainty in the temperature is 0.005 K, in the pressure is 0.01% of full range (0.00014 MPa for the low-pressure transducer, or 0.007 MPa for the high pressure transducer), in the

phase density is 0.17 $kg \cdot m^{-3}$, and in the vapor composition is 0.005 mole fraction.

ACKNOWLEDGMENT

This work was supported in part by the United States Department of Energy, Division of Engineering and Geosciences, Office of Basic Energy Sciences.

REFERENCES

1. V. Niesen, *J. Chem. Thermodyn.* **21**:915 (1989).
2. C. D. Holcomb and S. L. Outcalt, *Fluid Phase Equil.* **150**–**151**:815 (1998).
3. B. Younglove, *J. Phys. Chem. Ref. Data* **11** (Supl. 1) (1982).
4. P. G. Hill, *J. Phys. Chem. Ref. Data* **19**:1233 (1990).
5. R. C. Pemberton and C. J. Mash, *J. Chem. Thermodyn.* **10**:867 (1978).
6. D. Ambrose and C. H. S. Sprake, *J. Chem. Thermodyn.* **2:**631 (1970).
7. D. Ambrose, C. H. S. Sprake, and R. Townsend, *J. Chem. Thermodyn.* **7**:185 (1975).
8. I. Cibulka, *Fluid Phase Equil.* **89**:1 (1993).
9. I. Cibulka and M. Zikova, *J. Chem. Eng. Data* **39**:876 (1994).
10. J. L. Hales and J. H. Ellender, *J. Chem. Thermodyn.* **8**:1177 (1976).
11. H. Kubota, Y. Tanaka, and T. Makita, *Int. J. Thermophys.* **8**:47 (1987).
12. T. F. Sun, C. A. Ten Seldam, P. J. Kortbeek, N. J. Trappeniers, and S. N. Biswas, *Phys. Chem. Liq.* **18**:107 (1988).
13. Y. Takiguchi and M. Uematsu, *J. Chem. Thermodyn.* **28**:7 (1996).
14. R. Stryjek and J. H. Vera, *Can. J. Chem. Eng.* **64**:323 (1986).
15. D. S. H. Wong and S. I. Sandler, *AIChE J.* **38**:671 (1992).